Macromolecules

ARTICLE

pubs.acs.org/Macromolecules

Parent *o*-Phenylene Oligomers: Synthesis, Conformational Behavior, and Characterization

Sanyo M. Mathew and C. Scott Hartley*

Department of Chemistry & Biochemistry, Miami University, Oxford, Ohio 45056, United States

Supporting Information

ABSTRACT: The *o*-phenylenes are an unusual class of conjugated polymer, defined largely by substantial steric twisting along their backbones. Consequently, they exhibit limited conjugation but also interesting conformational behavior: they have been shown to adopt well-defined helical secondary structures, both in the solid state and in solution. While several examples of functionalized *o*-phenylene oligomers have been reported, most of the basic properties of the parent compounds are unknown. Here we report the synthesis and characterization of the series of unsubstituted *o*-phenylene oligomers up to the octamer. Through a combination of NMR spectroscopy, including dynamic NMR (EXSY), and computational chemistry, we have found that these compounds adopt compact helical conformations in solution with three repeat units per turn. Although formally conjugated, the oligomers have a very short effective conjugation length of $n_{ecl} \approx 4$ (based on UV−vis spectra), significantly shorter than most other conjugated systems. Also, unlike other (substituted) *o*-phenylenes, no hypochromicity is observed in their UV−vis spectra. The fluorescence spectra of the series exhibit a systematic blue shift with increasing length. We believe this unusual property results from increased steric congestion in the longer oligomers, which are therefore less able to accommodate structural relaxation in the excited state.

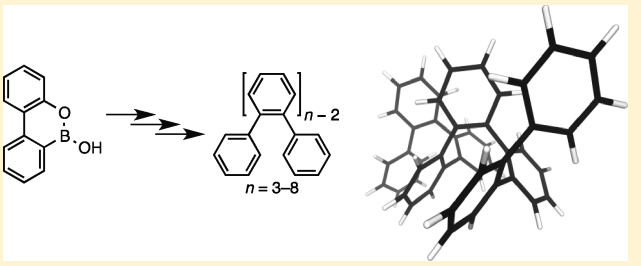

INTRODUCTION

o-Phenylenes represent a simple, fundamental class of conjugated polymers.[1] They are isomers of the *p*-phenylenes, now well-established as conducting films (when doped),[2] blue-emitting materials,[3,4] and single-molecule wires.[5,6] Similarly, the isomeric *m*-phenylenes have been studied as helical polymers and oligomers.[7−11] In contrast, the *o*-phenylenes have received little attention, and their properties are only now beginning to be investigated. Their defining characteristic is the substantial steric congestion along their backbones, which necessitates highly twisted conformational states. Presumably, this steric hindrance is why they were largely ignored: they are relatively difficult to synthesize by conventional aryl−aryl bond-forming methods, and π-overlap between repeat units is limited.[1,12] Consequently, their properties are not particularly desirable in the context of conjugated polymers for thin-film electronics. However, the *o*-phenylenes do have some interesting potential applications. In principle, they could be oxidatively planarized to give very narrow graphene nanoribbons, although they tend to rearrange under the standard reaction conditions for oxidative cyclodehydrogenation.[13] Perhaps more interestingly, the steric interactions along the backbone can produce well-defined conformational behavior, leading to applications as three-dimensional scaffolds and promoting through-space overlap between repeat units.

As early as the 1960s, Kovacic reported the syntheses of some *o*-phenylene polymers,[14−16] but the resulting materials received little subsequent characterization and were thought to contain structural defects (triphenylene moieties). More recently, electropolymerization of catechol derivatives was reported to yield poly(*o*-phenylenes),[17−19] but these materials were subsequently found to be small-molecule triphenylene derivatives.[20] Before 2010, there were three reports of series of *o*-phenylene oligomers of which we are aware:[21] by Wittig,[22] Ibuki and Ozasa,[23−26] and Simpkins.[27] However, these compounds were not studied in detail, and most of their basic properties were not reported.

Recently, we decided to investigate the series of methoxy-substituted *o*-phenylene oligomers **oP(OMe)^n** (n = 4−12).[28,29] We found that these compounds exhibit weak but surprisingly long-range conjugation: as n increases, a relatively small overall bathochromic shift of the UV−vis spectra is observed; however, significant changes are observed even for long oligomers, giving an effective conjugation length of n_{ecl} = 8.[28] Unusually, the **oP(OMe)^n** series also exhibits a systematic hypsochromic shift in their fluorescence spectra with increasing n. Using a combination of NMR spectroscopy and ab initio calculations, we found that these compounds adopt helical conformations in solution, with some disorder at their ends.[29] Simultaneously, Fukushima and Aida reported a series of *o*-phenylene oligomers up to the [48]-mer.[30] Remarkably, an octamer exhibits spontaneous deracemization in the solid state. The helical compound racemizes rapidly

Received: August 15, 2011
Revised: September 21, 2011
Published: October 11, 2011

Scheme 1[a]

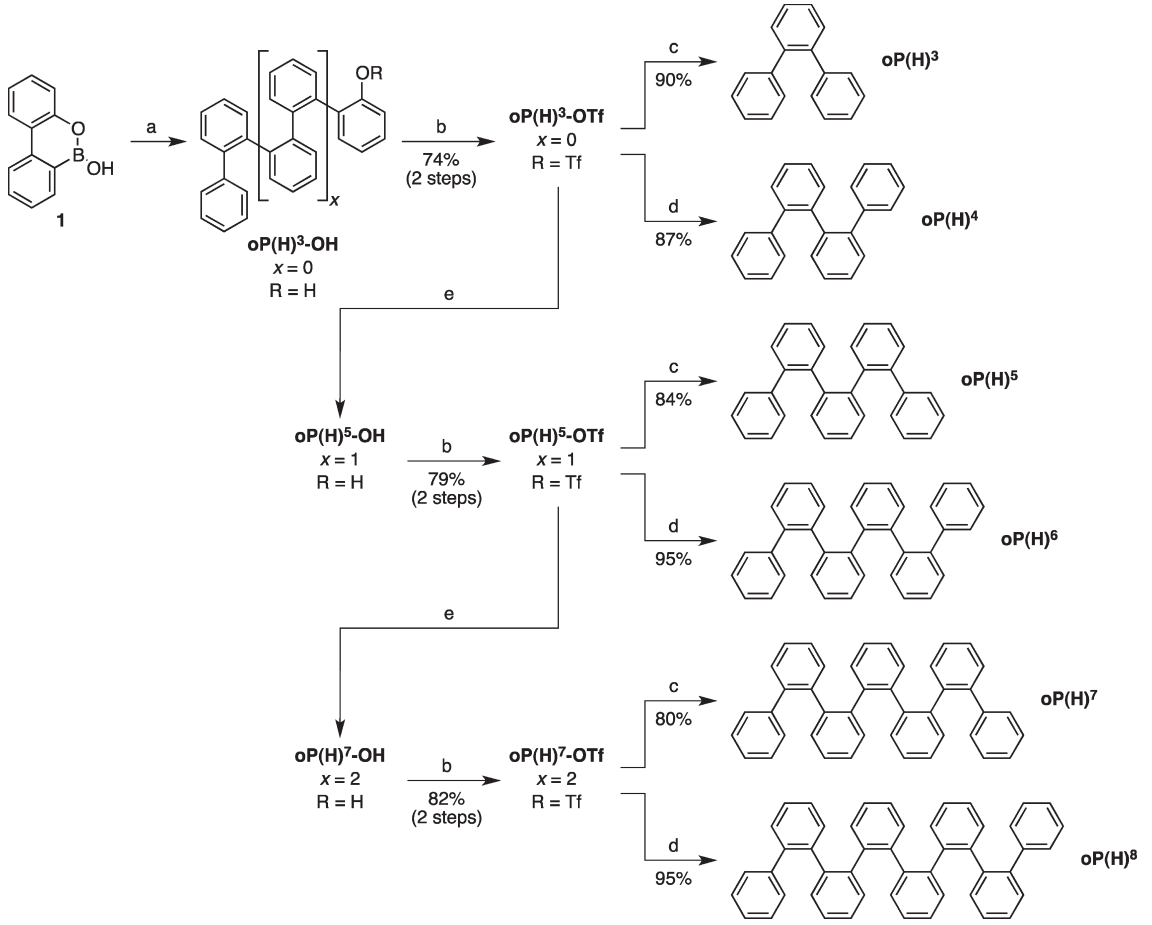

[a] Reagents and conditions: (a) iodobenzene, $Pd(OAc)_2$, SPhos, K_3PO_4, THF/H_2O (4/1), Δ; (b) Tf_2O, pyridine, DCM; (c) Mg, NH_4Cl, Pd/C, MeOH; (d) phenylboronic acid, $Pd(OAc)_2$, SPhos, K_3PO_4, THF/H_2O (4/1), Δ; (e) **1**, $Pd(OAc)_2$, SPhos, K_3PO_4, THF/H_2O (4/1), Δ.

in solution, but this process slows considerably on oxidation, which causes the springlike oligomer to compress.

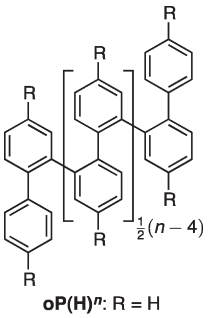

oP(H)^n: R = H
oP(OMe)^n: R = OMe

With the emerging interest in *o*-phenylenes, we realized that little was known about the parent (unsubstituted) series **oP(H)^n**. Unlike their *para* isomers, unsubstituted *o*-phenylenes should exhibit workable solubility even for the higher oligomers,[1,12] enabling convenient spectroscopic characterization. Many of these compounds are known in the literature.[22−26] However, to our knowledge, most of the basic properties of the **oP(H)^n** series, such as their NMR and fluorescence spectra, have not been reported, nor have modern techniques been used to determine their conformational behavior. Moreover, the reported syntheses are low yielding and not well-suited to the preparation of more complex *o*-phenylene-based compounds. Reexamination of this series is therefore needed to develop improved synthetic methods and establish baseline properties for the *o*-phenylenes as a class of conjugated oligomers and polymers.

RESULTS AND DISCUSSION

Synthesis. We desired a unified synthetic approach that allows the stepwise synthesis of oligomers of arbitrary length, that takes advantage of modern developments in aryl−aryl cross-coupling reactions, and that would be amenable to the future synthesis of oligomer heterosequences. Thus, we adapted our previous synthetic strategy for the **oP(OMe)^n** series.[28] Our approach, shown in Scheme 1, is based on Manabe's strategy for oligophenylene synthesis,[31,32] which uses phenols as masked triflates to control an iterative sequence of Suzuki−Miyaura coupling reactions.

The key monomer for this series is boroxarene **1**, which is readily obtained by treatment of commercially available 2-phenylphenol with BCl_3.[33] Suzuki−Miyaura coupling of **1** with iodobenzene using $Pd(OAc)_2$ and SPhos[34] gives hydroxy-functionalized *o*-phenylene trimer **oP(H)^3-OH**, which is then converted to the corresponding triflate **oP(H)^3-OTf**. At this point, the oligomer can be terminated by reductive deoxygenation[35]

dx.doi.org/10.1021/ma201866p |*Macromolecules* 2011, 44, 8425–8432

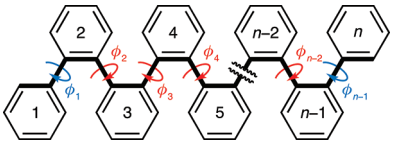

Figure 1. Labeling of dihedral angles (ϕ_i) in an *o*-phenylene.

(giving **oP(H)^3**) or by coupling to phenylboronic acid (giving **oP(H)^4**). Extension of the oligomer is accomplished by coupling to another equivalent of **1**, affording **oP(H)^5-OH**. These steps can then be repeated to prepare the higher oligomers. The isolated yields are uniformly high, and even the longest oligomers (**oP(H)^7** and **oP(H)^8**) were obtained in only eight steps from commercially available starting materials. We also note that this approach offers a straightforward method for the preparation of end-functionalized *o*-phenylenes by varying the coupling partners for the first and last steps.

All of the compounds in Scheme 1 exhibit good solubility in organic solvents. However, we were unable to synthesize oligomers longer than the octamer due to the poor solubility of the hydroxyl- or triflate-substituted nonamer intermediates. Thus, as we were unable to prepare any unfunctionalized oligomer longer than **oP(H)^8**, we cannot say at this point whether insolubility beyond $n = 8$ is an intrinsic property of the target compounds themselves. Nevertheless, the unsubstituted *o*-phenylenes are substantially more soluble than their *p*-phenylene analogues, which exhibit poor solubility beyond the heptamer even when functionalized with large branched alkyl solubilizing groups.[6] The increased solubility reflects the twisting of the *o*-phenylene backbone, which should prevent extensive $\pi-\pi$ contacts in the solid state. Melting points for the series were measured by differential scanning calorimetry (Table S1 and Figure S1) and show a slight odd−even effect.

Conformational Analysis. One of the most interesting aspects of the *o*-phenylenes is their conformational behavior. Previously, we reported a complete conformational analysis of the **oP(OMe)^n** series,[29] which should be applicable to the *o*-phenylenes in general. Briefly, the overall conformation of an *o*-phenylene oligomer is dictated by the internal torsional angles $\phi_2-\phi_{n-2}$, shown in Figure 1. (The terminal torsional angles, ϕ_1 and ϕ_{n-1}, do not need to be considered as rotation about these bonds is degenerate.) On the basis of computational modeling, we found that each of these dihedrals can assume one of four possible values: $\phi_i \approx \pm 70°$ or $\pm 130°$. However, because of coupling along the backbone, the total conformational pool can be divided into two separate enantiomeric subsets: within a single molecule, each ϕ_i can assume one of only two possible values, either $\phi_i \approx +70°/-130°$ or $\phi_i \approx -70°/+130°$. Here we discuss and visualize the oligomers in terms of the $-70°/+130°$ set, but we stress that we have not resolved any of these compounds; thus, all structures presented represent racemates. To distinguish different conformers, we label bonds in the $-70°$ state "A" and those in the $+130°$ state "B" (e.g., the "AB" conformer of **oP(H)^5** has $\phi_2 \approx -70°$ and $\phi_3 \approx +130°$).

Even with the constraint that each ϕ_i can assume only two possible states within a single molecule, there is, in principle, a large number of available conformers for an *o*-phenylene oligomer.[36] However, it is illustrative to consider the two possible limiting cases. If all $\phi_i \approx -70°$ (the A_{n-3} conformer), then the oligomer's conformation can be described as a compact, closed helix, with offset, coplanar stacking of every third monomer.

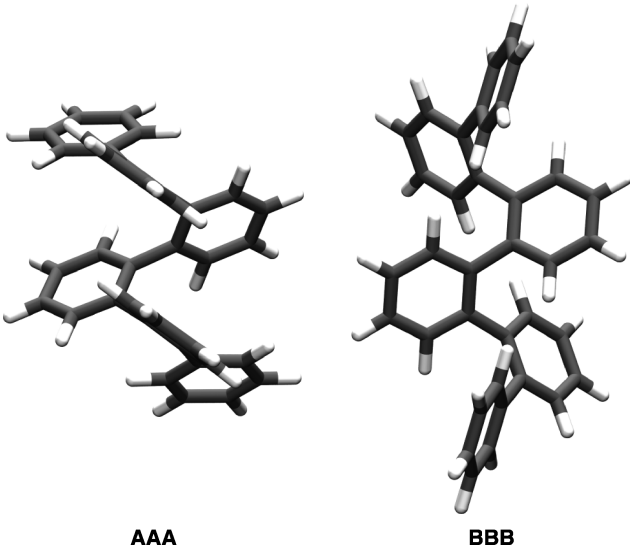

Figure 2. Closed helical (AAA, left) and open helical (BBB, right) conformers of **oP(H)^6**. Geometries optimized at the BH&HLYP/6-31+G(d,p) level.

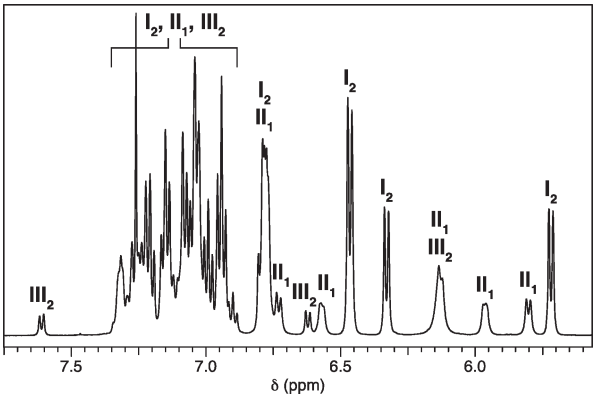

Figure 3. ^{1}H NMR of **oP(H)^6** (500 MHz, $CDCl_3$, −5 °C). Selected signals corresponding to conformers $\mathbf{I_2}$, $\mathbf{II_1}$, and $\mathbf{III_2}$ are labeled. The remaining (overlapping) signals can be separated and assigned based on 2D spectra; assignments are tabulated in the Supporting Information.

Conversely, if all $\phi_i \approx +130°$ (the B_{n-3} conformer), then the oligomers are in an extended, open helical conformation without intramolecular stacking. These two conformers are illustrated in Figure 2 for **oP(H)^6**. The specific conformational state of the *o*-phenylenes is important. Aromatic repeat units in the open conformer are closer to coplanarity and thus should exhibit more significant π-system delocalization. The closed conformer has more interesting spatial correlations between repeat units as every third aromatic ring is closely stacked.

Several reported crystal structures of *o*-phenylene oligomers have suggested that they are predisposed to closed helical conformations (A_{n-3}) in the solid state.[27,28,30] However, given the complexity of the conformational pool, it was not clear if they adopted these well-defined three-dimensional structures in solution (as opposed to a large number of random coil conformations). Using a combination of NMR spectroscopy and computational chemistry (see below), we demonstrated[29] that our previous series of *o*-phenylenes (**oP(OMe)^n**) exist primarily

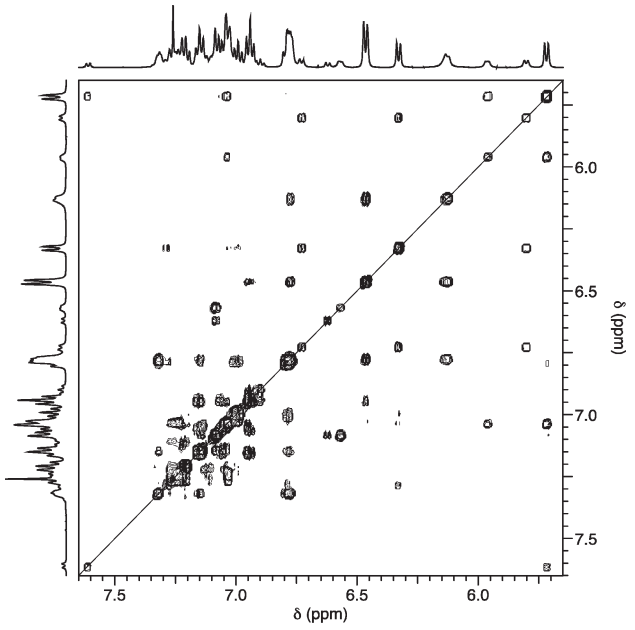

Figure 4. EXSY spectrum of **oP(H)^6** (500 MHz, $CDCl_3$, −5 °C, t_m = 0.5 s).

in the stacked helical conformations (A_{n-3}) in solution, with some minor conformers identified that had defects (B states) only at the very ends. These results suggest that *o*-phenylenes may have an important role to play as scaffolds for the positioning of substituents in space. However, considering the limited number of reported examples of *o*-phenylene oligomers, most of which have been functionalized with electron-donating groups, the conformational behavior of the class as a whole, independent of substituent effects, was not clear.

Similar to **oP(OMe)^n**, the unsubstituted **oP(H)^n** exhibit complex NMR spectra at room temperature (and below) for $n \geq 5$. As a representative example, here we discuss **oP(H)^6** in detail, as it gives the most complete data set. Its ^{1}H NMR spectrum at −5 °C is shown in Figure 3 (the spectrum is similar at room temperature, but with slightly broadened signals). Remarkably, although this compound consists only of unsubstituted benzene rings, the ^{1}H chemical shifts span >2 ppm, presumably due to the high density of aromatic π-systems and their associated ring currents.

At first inspection, it would appear that the sample of **oP(H)^6** is contaminated with significant amounts of impurities given the large number of small signals with nonintegral relative areas. However, as we previously demonstrated for the methoxy-substituted series, these smaller signals are due to minor conformational states in slow exchange on the NMR time scale. This is demonstrated in the EXSY (i.e., NOESY) NMR spectrum, shown in Figure 4. All of the minor signals exhibit cross-peaks with corresponding major signals. These cross-peaks are of the same phase as the diagonal; since this is a small molecule, they must therefore arise from chemical exchange (and not through-space NOESY effects). Using the EXSY spectrum, the NMR signals can be assigned to three exchanging conformers. The major conformer, $\mathbf{I_2}$, is 2-fold symmetric. There are then two minor conformers: one, $\mathbf{II_1}$, which is nonsymmetric and one, $\mathbf{III_2}$, which is 2-fold symmetric. Conformers $\mathbf{I_2}$, $\mathbf{II_1}$, and $\mathbf{III_2}$ have relative populations of 49:42:10 based on the integration of well-separated signals (and accounting for their relative symmetries).

In order to associate these experimentally observed conformers with specific molecular geometries, we undertook to completely assign their ^{1}H chemical shifts. Our strategy[29] was to first obtain a complete set of assignments for the major conformer ($\mathbf{I_2}$) using a standard set of two-dimensional NMR experiments (DQFCOSY, HMQC, and HMBC). Because the signals corresponding to $\mathbf{I_2}$ are significantly more intense than the others (due to both its greater population and higher symmetry), they are readily identified in the contour plots of the 2D spectra. With the assignments for $\mathbf{I_2}$ in hand, we then used the EXSY spectrum (in combination with weak COSY signals) to map them onto the minor conformers. In this way we obtained a nearly complete set of ^{1}H chemical shifts for $\mathbf{III_2}$.[37] Because $\mathbf{II_1}$ has lower symmetry than $\mathbf{I_2}$, it is impossible to unambiguously assign the corresponding rings on either side of the oligomer (i.e., rings 1 vs 6, 2 vs 5, and 3 vs 4). Instead, we were able to obtain (nearly) complete sets of chemical shifts for each of the six individual rings, but their connectivity was determined according to the best match to the spectra computed by DFT (see below).

Because each of ϕ_2, ϕ_3, and ϕ_4 of **oP(H)^6** can assume either the A (−70°) or B (+130°) states, there are a total of six possible conformers: four that are C_2-symmetric (AAA, BAB, ABA, BBB) and two that are unsymmetric (AAB and ABB). For comparison with the experimental chemical shifts, we then carried out DFT geometry optimizations of each of these conformers (in the gas phase). We chose the BH&HLYP/6-31+G(d,p) level since this functional should better estimate the strength of $\pi-\pi$ stacking interactions;[38] in any event, we did not observe any significant differences in the performance of BH&HLYP compared to more common methods (e.g., B3LYP). After geometries were obtained for each of the six conformers, shown in Figure 5 and Figure S2, ^{1}H chemical shifts were calculated using the GIAO method[39,40] at the PCM/WP04/6-31G(d) level,[41] which has been shown to be an efficient and economical approach to the ab initio prediction of ^{1}H NMR spectra in chloroform.[42] We then compared the sets of calculated chemical shifts for our six possible conformers with the experimental data for $\mathbf{I_2}$, $\mathbf{II_1}$, and $\mathbf{III_2}$. As a figure of merit, we chose the root-mean-squared (rms) error of the calculated chemical shift (δ_{calc}) against the experimental chemical shift (δ_{expt}), scaled according to a linear fit between the two data sets.[43]

All three experimentally observed conformers were thus readily assigned to one specific three-dimensional geometry. The good matches all had rms errors less than 0.16 ppm, and bad matches had rms errors greater than 0.44 ppm. These thresholds are in good agreement with the established errors for the method based on a set of test molecules (0.12 ppm).[42] Based on this analysis, $\mathbf{I_2}$ is AAA, $\mathbf{II_1}$ is AAB, and $\mathbf{III_2}$ is BAB; the plots of the calculated against experimental NMR data are given in Figure 5. The three identified conformers are directly analogous to those observed for **oP(OMe)^6**.[29] The conformer distribution is similar but slightly different: 49:42:10 for **oP(H)^6** compared to 55:36:10 for **oP(OMe)^6**. Notably, of the six possible backbone conformations, only those with the central bond in the "A" state are observed ($\phi_3 \approx -77.5°$, −73.9°, and −82.0° for AAA, AAB, and BAB, respectively).

We then sought to extend our NMR analysis to the other members of the **oP(H)^n** series. **oP(H)^4**, as expected, exists in rapid conformational exchange near room temperature and thus exhibits a standard first-order NMR spectrum. For **oP(H)^5**, while

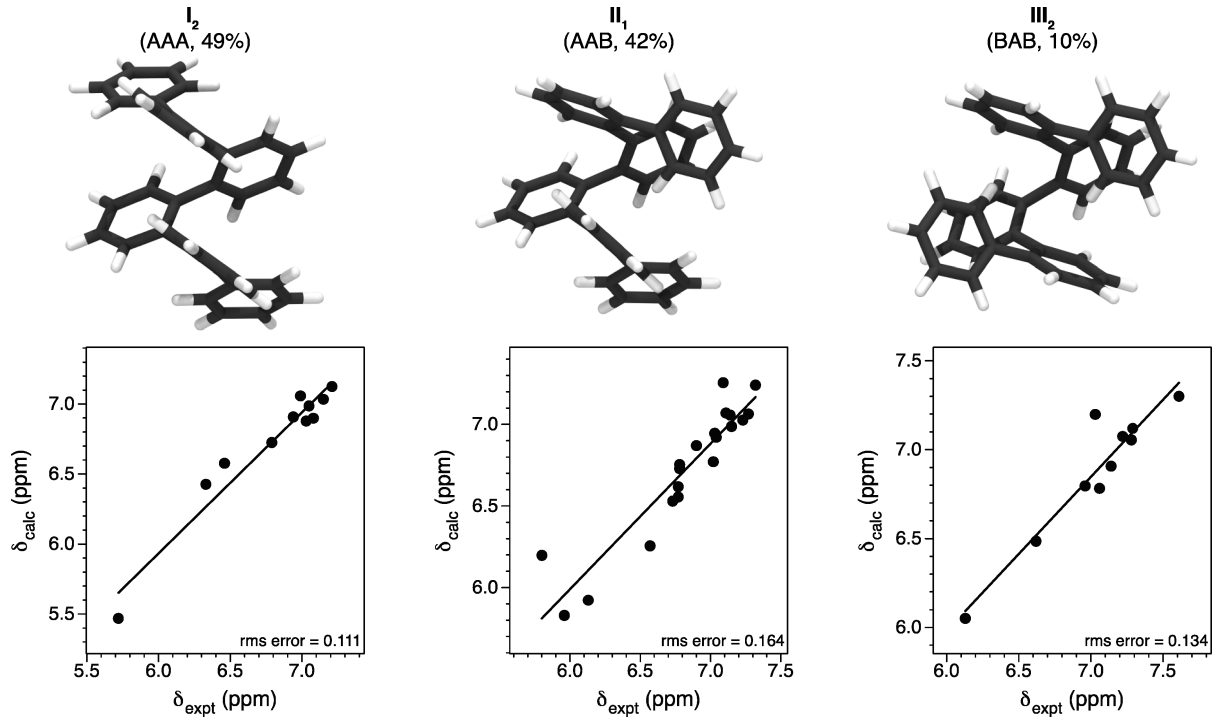

Figure 5. Geometry-minimized conformers for **oP(H)**^{6} and plots of calculated vs experimental ^{1}H chemical shifts.

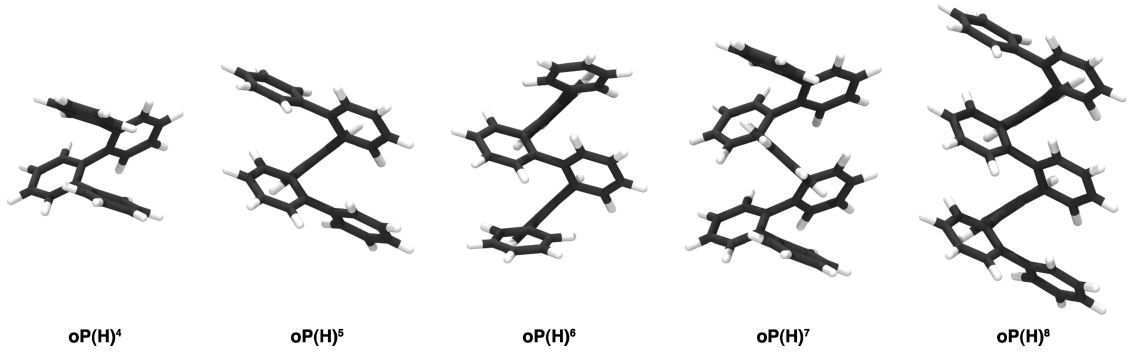

Figure 6. Closed helical (A_{n-3}) conformers for the **oP(H)**^{n} series, minimized at the BH&HLYP/6-31+G(d,p) level.

there is some evidence for slow exchange at 0 °C (a few small signals in the ^{1}H NMR spectrum and associated EXSY cross-peaks), the data cannot be completely assigned to multiple independent conformers, suggesting that there are still significant backbone rearrangements that are rapid on the NMR time scale. Like **oP(H)**^{6}, the longer oligomers **oP(H)**^{7} and **oP(H)**^{8} exist in a slow exchange regime. For these oligomers, we were able to obtain chemical shift assignments for the major conformer in solution, which is 2-fold symmetric in both cases. Unfortunately, although EXSY spectroscopy indicates that the minor signals in the spectra of **oP(H)**^{7} and **oP(H)**^{8} result from less-populated conformational states, we were unable to map assignments for the major conformer onto the minor conformers due to the considerable signal overlap. This is perhaps not surprising, as the **oP(H)**^{n} series represents the worst case for this NMR analysis strategy, with the largest possible number of aromatic signals and no signal separation from substituent effects.

For **oP(H)**^{7} and **oP(H)**^{8}, the experimental chemical shift data for the major conformer are in good agreement with that calculated for the closed helical A_{n-3} conformers (rms errors $\leq$0.11 ppm, Figure S3). We therefore conclude that the **oP(H)**^{n} series adopts stacked helical conformations in solution, shown in Figure 6. On the basis of the results for **oP(H)**^{6}, and by analogy with our results for the **oP(OMe)**^{n} series, it seems likely that conformational disorder occurs primarily at the ends of the oligomers. Consequently, we conclude that the preference for stacked helical conformations is a basic property of simple *o*-phenylenes. Further studies will be needed to determine the role of substituent effects in controlling the conformational state of the oligomers. However, considering the similar behavior of **oP(H)**^{n} compared to **oP(OMe)**^{n}, it appears at this point that substituents do not have a dramatic effect on the conformational distribution.

In contrast to our *o*-phenylenes, Ito has investigated a series of structurally related poly(2,3-quinoxalines), many of which adopt

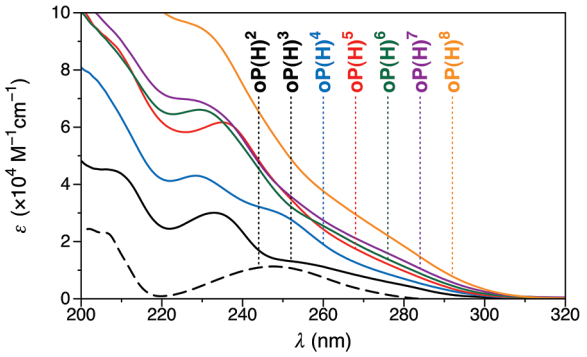

Figure 7. UV−vis spectra (cyclohexane) of **oP(H)^n** (n = 2−8).

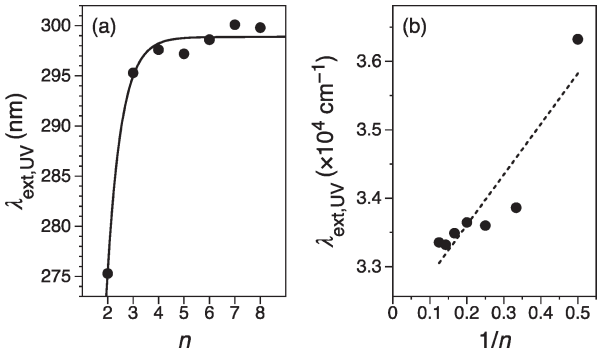

Figure 8. Plots of the extrapolated UV−vis onset vs (a) n or (b) $1/n$. The solid line in (a) is a fit to eq 1 (χ^2 = 5.39).

conformations analogous to the open B_{n-3} conformers.[44−46] However, the 2,3-quinoxaline repeat units in these oligomers lack the hydrogen atoms *ortho* to the biaryl bonds and thus should be better able to accommodate a more planar conformation; further, these polymers are typically functionalized with very bulky substituents (e.g., tolyl), which likely bias the compounds toward the open helix through steric interactions. Interestingly, oligo(2,3-naphthalenes) lacking the bulky substituents exhibit closed helical conformations similar to those observed for the *o*-phenylenes.[47]

UV−vis Spectroscopy. Although the UV−vis spectra of several members of the **oP(H)^n** series have been reported,[24] they have not been analyzed in detail. The UV−vis spectra of the complete **oP(H)^n** series (n = 2−8) are shown in Figure 7; the spectra for the known members of the series are in agreement with those previously reported. The spectra show no solvatochromism, as indicated by comparisons of spectra of cyclohexane and dichloromethane solutions (Figure S4), nor are their shapes affected by concentration. Curiously, while the **oP(OMe)^n** series exhibits a substantial hypochromic effect in its UV−vis spectra (i.e., when normalized for n, ε decreases with increasing n), we observe no significant hypochromicity for the **oP(H)^n** series (Figure S4). As hypochromicity is associated with well-ordered arrangements of chromophore transition dipole moments,[48] its absence either suggests less rigid conformational ordering for **oP(H)^n** or reflects the different polarizations of the transitions.

Inspection of the UV−vis spectra clearly indicates a significant red shift as the oligomer is extended from **oP(H)^2** (biphenyl) to **oP(H)^3**; however, the change in spectra attenuates sharply for n > 3. More quantitatively, the degree of conjugation in a conjugated oligomer (or polymer) may be evaluated in terms of the effective conjugation length n_{ecl}. The effective conjugation length can be determined from a plot of the UV−vis transitions against n using an empirical method developed by Meier:[49]

$$\lambda_{n,\mathrm{UV}} = \lambda_{\infty,\mathrm{UV}} - \Delta\lambda_{\mathrm{UV}}\, e^{-b(n-1)} \qquad (1)$$

where $\lambda_{n,UV}$ is the low-energy absorption maximum for an oligomer with n monomer units. The parameter $\lambda_{\infty,UV}$ is simply $\lambda_{n,UV}$ extrapolated to the polymer limit, $\Delta\lambda_{UV} = \lambda_{\infty,UV} - \lambda_{1,UV}$ is the overall effect of conjugation, and b is the extent of conjugation. If we define the effective conjugation length as the value of n for which $\lambda_{\infty,UV} - \lambda_{n,UV} \leq 1$ nm, it follows that

$$n_{ecl} = \frac{\ln \Delta\lambda_{\mathrm{UV}}}{b} + 1 \qquad (2)$$

For the **oP(H)^n** oligomers (n > 2), we unfortunately do not have well-defined peaks in the low-energy regions of the spectra. Accordingly, we have adopted the same approach we used to analyze the **oP(OMe)^n** series, evaluating the change in the extrapolated UV−vis absorption onset $\lambda_{ext,UV}$.[50] Meier has shown that this provides functionally the same results,[49] and we have confirmed that it is equivalent to the use of absorption maxima for other conjugated oligomers (e.g., *p*-phenylenes),[6] allowing meaningful comparison with n_{ecl} values for other classes of compounds.

A plot of $\lambda_{ext,UV}$ against n is shown in Figure 8a. A fit to eq 1 yields $\Delta\lambda_{UV}$ = 142 ± 47 nm, $\lambda_{\infty,UV}$ = 298.88 ± 0.57 nm, and b = 1.79 ± 0.33. From these parameters, $n_{ecl} \approx 4$. The small effective conjugation length for **oP(H)^n** is also obvious when $\lambda_{ext,UV}$ is plotted against $1/n$, as shown in Figure 8b. For most conjugated oligomers, a good linear relationship is observed between $\lambda_{ext,UV}$ and $1/n$ at low n, with a break from linearity around n_{ecl}. However, for the **oP(H)^n** series, the data are not adequately fit by a linear function, even for n = 2−4, reflecting the very short n_{ecl} for the parent *o*-phenylenes and consistent with the value of $n_{ecl} \approx 4$ obtained using eqs 1 and 2.

Compared to other classes of conjugated oligomers, the unsubstituted *o*-phenylenes, perhaps not surprisingly, have a short effective conjugation length, roughly comparable to certain phenylene ethynylenes or sterically hindered polypyroles.[49,51] For comparison, for unsubstituted *p*-phenylenes[3,49] $n_{ecl} \approx 10$ (if planarity is forced along the backbone $n_{ecl} \geq 12$).[52−54] These values may in fact represent significant underestimates of n_{ecl} for *p*-phenylenes, given recent results which question its determination based on the extrapolation of UV−vis data (particularly the $1/n$ dependence).[55] Nevertheless, the value of $n_{ecl} \approx 4$ for the **oP(H)^n** series should be accurate as we have used Meier's approach (i.e., eqs 1 and 2 rather than plots of UV data vs $1/n$) and especially considering that we have synthesized oligomers longer than the saturation point of the UV−vis data. The short n_{ecl} of the *o*-phenylenes is reasonable in view of the large twisting of the *o*-phenylene backbone, which would be expected to attenuate conjugation. However, the effective conjugation length of the **oP(H)^n** series is significantly less than that of the **oP(OMe)^n** series ($n_{ecl} \approx 8$). In our original paper on the **oP(OMe)^n** series, we attributed their low $\Delta\lambda$ (= 39 nm) to the twisting of their π-systems and their long n_{ecl} to conformational rigidity. For our current series of compounds, $\Delta\lambda$ is much larger than for the methoxy-substituted case, although the large experimental uncertainty for this parameter makes it difficult to draw firm conclusions as to the cause. However, while the global conformational distribution is essentially the same for the two sets of oligomers (reflected in the similar populations of **I_2**, **II_1**, and **III_2**), it is possible that the conformational rigidity is reduced for the

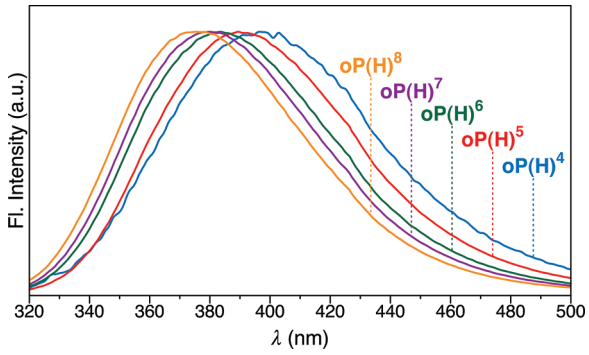

Figure 9. Steady-state fluorescence spectra of **oP(H)^n** (cyclohexane).

Table 1. Fluorescence Properties of oP(H)^n in Cyclohexane

	$\lambda_{max,FL}$ (nm)	Φ_f	τ_f (ns)	k_r ($\times 10^7$ s^{-1})	k_{nr} ($\times 10^7$ s^{-1})
oP(H)^4	396.5	0.01	0.4[a]		
oP(H)^5	390.5	0.13	3.3	3.9	26
oP(H)^6	383.0	0.11	3.8	2.9	23
oP(H)^7	380.0	0.17	5.8	2.9	14
oP(H)^8	376.0	0.18	6.0	3.0	14

[a] Biexponential fit: 0.4 ns (97.7%), 6.8 ns (2.3%).

oP(H)^n series, possibly due to reduced $\pi-\pi$-type interactions between the monomers. A looser, less well-defined conformational state for the **oP(H)^n** series could explain the reduced n_{ecl}. Greater conformational flexibility is also consistent with the lack of hypochromicity in the UV−vis spectra of **oP(H)^n**, which was quite pronounced for **oP(OMe)^n** (up to 60%).

Fluorescence Spectroscopy. Beyond $n = 3$, the unsubstituted *o*-phenylenes are fluorescent, as shown in Figure 9. Despite the expected attenuated conjugation for the *o*-phenylenes, the emission maximum for **oP(H)^4** is actually red-shifted compared to the analogous *p*-quaterphenyl (396 vs 365 nm).[56] Like the UV−vis spectra, the shapes of the fluorescence spectra are found to be independent of concentration and solvent (Figure S5). Excitation spectra are in good agreement with the UV−vis spectra (Figure S6). Quantum yields were measured relative to 9,10-diphenylanthracene ($\Phi_f = 0.91$)[57] and are tabulated in Table 1. While **oP(H)^3** is essentially nonfluorescent (Φ_f could not be determined on our instruments), the quantum yields increase with increasing length and plateau around 0.18, which is identical to the reported quantum yield of biphenyl (0.18).[56,58] This behavior is very similar to the behavior of the **oP(OMe)^n** series (e.g., for **oP(OMe)^8**, $\Phi_f = 0.19$). Fluorescence lifetimes (τ_f) were determined by time-correlated single photon counting in degassed cyclohexane. The lifetimes increase with increasing chain length, although in all cases are substantially less than that of biphenyl (16 ns).[58] Radiative rate constants ($k_r = \Phi_f \tau_f^{-1}$) fall to a constant limiting value of 3×10^7 s^{-1} for $n \geq 6$, whereas nonradiative rate constants ($k_{nr} = (1 - \Phi_f)\tau_f^{-1}$) appear to fall to a limiting value of 14×10^7 s^{-1} for $n \geq 7$.

The fluorescence spectra exhibit a small but systematic *hypsochromic* shift with increasing length, with a overall shift of about 20 nm from **oP(H)^4** to **oP(H)^8**. While changes in the UV−vis spectra reach saturation quite quickly ($n_{ecl} \approx 4$), even for **oP(H)^7** and **oP(H)^8** there is a significant difference in the fluorescence maxima. As we had previously observed similar behavior for the **oP(OMe)^n** series, the blue shift in fluorescence spectra with increasing length appears to be an unusual but general feature of the *o*-phenylenes. This behavior is not exhibited by most conjugated oligomers, with the exception of certain donor−acceptor-substituted compounds for which extension of the chain length attenuates a charge-transfer interaction. The **oP(H)^n** series clearly should not exhibit charge-transfer states (nor do we observe any solvatochromism in either the UV−vis or fluorescence spectra). Since analogous hypsochromic shifts are not observed in the UV−vis spectra of the oligomers, this effect must originate from varying degrees of structural rearrangements in the excited states, leading to reduced Stokes shifts. This phenomenon therefore must result from the unusual conformational behavior of the *o*-phenylenes compared to most other conjugated oligomers. It is well-known that the *p*-phenylenes undergo planarization in the excited state.[59,60] Clearly, for a stacked helical *o*-phenylene this is not possible. We speculate at this point that the shorter oligomers must be better able to accommodate reductions in ϕ_i in the excited state due to reduced steric hindrance. We are currently undertaking time-dependent DFT investigations of the excited-state properties of the **oP(H)^n** series in order to test this hypothesis.

CONCLUSIONS

We have developed an improved method for the synthesis of the parent *o*-phenylene oligomers **oP(H)^n** up to the octamer. Using NMR spectroscopy, we have shown that unsubstituted *o*-phenylenes predominantly adopt stacked helical conformations in solution. A more detailed analysis was possible for **oP(H)^6**, which adopts only three (of six) conformers, differing only in the orientation of the ends of the chain. The conformational distribution favors the stacked helical conformer and is similar to that of our previously reported methoxy-substituted **oP(OMe)^6**. Changes in the UV−vis spectra with length saturate quickly for the **oP(H)^n** series, which has an effective conjugation length of $n_{ecl} \approx 4$ (compared to $n_{ecl} \approx 8$ for **oP(OMe)^n**). Further, the UV−vis spectra do not exhibit increasing hypochromicity with increasing *n*. These behaviors may result from decreased conformational rigidity for **oP(H)^n**. The fluorescence spectra exhibit a hypsochromic shift with increasing length, an unusual feature for conjugated oligomers that we believe derives from inhibited excited-state structural relaxation for the longer oligomers.

ASSOCIATED CONTENT

Supporting Information. Supplementary figures referred to in the text; NMR spectra (1D and 2D); TCSPC data and fits; MALDI spectra; experimental procedures; and Cartesian coordinates of optimized geometries. This material is available free of charge via the Internet at http://pubs.acs.org.

AUTHOR INFORMATION

Corresponding Author
*E-mail: scott.hartley@muohio.edu.

ACKNOWLEDGMENT

Primary support from the National Science Foundation (CHE-0910477) is gratefully acknowledged. Gaussian 09 was purchased with the assistance of the Air Force Office of Scientific

Research (FA9550-10-1-0377), and the MALDI mass spectrometer was purchased with the assistance of the NSF (CHE-0839233).

REFERENCES

(1) Berresheim, A. J.; Müller, M.; Müllen, K. *Chem. Rev.* **1999**, *99*, 1747–1785.

(2) Ivory, D. M.; Miller, G. G.; Sowa, J. M.; Shacklette, L. W.; Chance, R. R.; Baughman, R. H. *J. Chem. Phys.* **1979**, *71*, 1506–1507.

(3) Grimsdale, A. C.; Müllen, K. *Adv. Polym. Sci.* **2006**, *199*, 1–82.

(4) Grimsdale, A. C.; Chan, K. L.; Martin, R. E.; Jokisz, P. G.; Holmes, A. B. *Chem. Rev.* **2009**, *109*, 897–1091.

(5) Weiss, E. A.; Ahrens, M. J.; Sinks, L. E.; Gusev, A. V.; Ratner, M. A.; Wasielewski, M. R. *J. Am. Chem. Soc.* **2004**, *126*, 5577–5584.

(6) Banerjee, M.; Shukla, R.; Rathore, R. *J. Am. Chem. Soc.* **2009**, *131*, 1780–1786.

(7) Goto, H.; Katagiri, H.; Furusho, Y.; Yashima, E. *J. Am. Chem. Soc.* **2006**, *128*, 7176–7178.

(8) Goto, H.; Furusho, Y.; Yashima, E. *J. Am. Chem. Soc.* **2007**, *129*, 9168–9174.

(9) Goto, H.; Furusho, Y.; Yashima, E. *J. Am. Chem. Soc.* **2007**, *129*, 109–112.

(10) Ben, T.; Goto, H.; Miwa, K.; Goto, H.; Morino, K.; Furusho, Y.; Yashima, E. *Macromolecules* **2008**, *41*, 4506–4509.

(11) Miwa, K.; Furusho, Y.; Yashima, E. *Nature Chem.* **2010**, *2*, 444–449.

(12) Tour, J. M. *Adv. Mater.* **1994**, *6*, 190–198.

(13) Ormsby, J. L.; Black, T. D.; Hilton, C. L.; Bharat; King, B. T. *Tetrahedron* **2008**, *64*, 11370–11378.

(14) Kovacic, P.; Uchic, J. T.; Hsu, L.-C. *J. Polym. Sci., Part A: Polym. Chem.* **1967**, *5*, 945–964.

(15) Kovacic, P.; Ramsey, J. S. *J. Polym. Sci., Part A: Polym. Chem.* **1969**, *7*, 111–125.

(16) Hsing, C.-F.; Jones, M. B.; Kovacic, P. *J. Polym. Sci., Part A: Polym. Chem.* **1981**, *19*, 973–984.

(17) Xu, J.; Liu, H.; Pu, S.; Li, F.; Luo, M. *Macromolecules* **2006**, *39*, 5611–5616.

(18) Ma, M.; Liu, H.; Xu, J.; Li, Y.; Wan, Y. *J. Phys. Chem. C* **2007**, *111*, 6889–6896.

(19) Dong, B.; Zheng, L.; Xu, J.; Liu, H.; Pu, S. *Polymer* **2007**, *48*, 5548–5555.

(20) Voisin, E.; Williams, V. E. *Macromolecules* **2008**, *41*, 2994–2997.

(21) Here, we consider only cases of oligomers in excess of six repeat units.

(22) Wittig, G.; Lehmann, G. *Chem. Ber.* **1957**, *90*, 875–892.

(23) Ibuki, E.; Ozasa, S.; Murai, K. *Bull. Chem. Soc. Jpn.* **1975**, *48*, 1868–1874.

(24) Ozasa, S.; Fujioka, Y.; Fujiwara, M.; Ibuki, E. *Chem. Pharm. Bull.* **1980**, *28*, 3210–3222.

(25) Ibuki, E.; Ozasa, S.; Fujioka, Y.; Kitamura, H. *Chem. Pharm. Bull.* **1980**, *28*, 1468–1476.

(26) Ibuki, E.; Ozasa, S.; Fujioka, Y.; Okada, M.; Yanagihara, Y. *Chem. Pharm. Bull.* **1982**, *30*, 2369–2379.

(27) Blake, A. J.; Cooke, P. A.; Doyle, K. J.; Gair, S.; Simpkins, N. S. *Tetrahedron Lett.* **1998**, *39*, 9093–9096.

(28) He, J.; Crase, J. L.; Wadumethrige, S. H.; Thakur, K.; Dai, L.; Zou, S.; Rathore, R.; Hartley, C. S. *J. Am. Chem. Soc.* **2010**, *132*, 13848–13857.

(29) Hartley, C. S.; He, J. *J. Org. Chem.* **2010**, *75*, 8627–8636.

(30) Ohta, E.; Sato, H.; Ando, S.; Kosaka, A.; Fukushima, T.; Hashizume, D.; Yamasaki, M.; Hasegawa, K.; Muraoka, A.; Ushiyama, H.; Yamashita, K.; Aida, T. *Nature Chem.* **2011**, *3*, 68–73.

(31) Ishikawa, S.; Manabe, K. *Chem. Commun.* **2006**, 2589–2591.

(32) Ishikawa, S.; Manabe, K. *Chem. Lett.* **2006**, *35*, 164–165.

(33) Zhou, Q. J.; Worm, K.; Dolle, R. E. *J. Org. Chem.* **2004**, *69*, 5147–5149.

(34) Walker, S. D.; Barder, T. E.; Martinelli, J. R.; Buchwald, S. L. *Angew. Chem., Int. Ed.* **2004**, *43*, 1871–1876.

(35) Sajiki, H.; Mori, A.; Mizusaki, T.; Ikawa, T.; Maegawa, T.; Hirota, K. *Org. Lett.* **2006**, *8*, 987–990.

(36) For an oligomer of length n, the number of possible conformations is $N = 2^{n-4} + 2^{(1/2)n-2}$.

(37) Unfortunately, because of spectral overlap, 1 of 11 protons of $\mathbf{III_2}$ and 2 of 22 protons of $\mathbf{II_1}$ could not be assigned. See the Supporting Information for details.

(38) Waller, M. P.; Robertazzi, A.; Platts, J. A.; Hibbs, D. E.; Williams, P. A. *J. Comput. Chem.* **2006**, *27*, 491–504.

(39) Ditchfield, R. *Mol. Phys.* **1974**, *27*, 789–807.

(40) Wolinski, K.; Hinton, J. F.; Pulay, P. *J. Am. Chem. Soc.* **1990**, *112*, 8251–8260.

(41) Wiitala, K. W.; Hoye, T. R.; Cramer, C. J. *J. Chem. Theory Comput.* **2006**, *2*, 1085–1092.

(42) Jain, R.; Bally, T.; Rablen, P. R. *J. Org. Chem.* **2009**, *74*, 4017–4023.

(43) Following the approach of Rablen and co-workers,[42] before calculating the error, we scale the δ_{calc} values according to $\delta_{calc}' = (\delta_{calc} - b)/m$, where m is the slope and b is the intercept from the plots in Figure 5. This is similar to the approach we took in our previous paper,[29] where we considered the standard error of the regression, except that it favors fits with slopes close to unity. Either method leads to the same conclusions.

(44) Ito, Y.; Ihara, E.; Murakami, M.; Sisido, M. *Macromolecules* **1992**, *25*, 6810–6813.

(45) Ito, Y.; Ohara, T.; Shima, R.; Suginome, M. *J. Am. Chem. Soc.* **1996**, *118*, 9188–9189.

(46) Ito, Y.; Miyake, T.; Hatano, S.; Shima, R.; Ohara, T.; Suginome, M. *J. Am. Chem. Soc.* **1998**, *120*, 11880–11893.

(47) Motomura, T.; Nakamura, H.; Suginome, M.; Murakami, M.; Ito, Y. *Bull. Chem. Soc. Jpn.* **2005**, *78*, 142–146.

(48) Bloomfield, V. A.; Crothers, D. M.; Tinoco, I., Jr. *Physical Chemistry of Nucleic Acids*; Harper & Row: New York, 1974.

(49) Meier, H.; Stalmach, U.; Kolshorn, H. *Acta Polym.* **1997**, *48*, 379–384.

(50) Zhao, Y.; Campbell, K.; Tykwinski, R. R. *J. Org. Chem.* **2002**, *67*, 336–344.

(51) Schumm, J. S.; Pearson, D. L.; Tour, J. M. *Angew. Chem., Int. Ed. Engl.* **1994**, *33*, 1360–1363.

(52) Grimsdale, A. C.; Müllen, K. *Adv. Polym. Sci.* **2008**, *212*, 1–48.

(53) Grimme, J.; Kreyenschmidt, M.; Uckert, F.; Müllen, K.; Scherf, U. *Adv. Mater.* **1995**, *7*, 292–295.

(54) Where applicable, the literature data have been reevaluated using eqs 1 and 2 for consistency.

(55) Wang, Q.; Qu, Y.; Tian, H.; Geng, Y.; Wang, F. *Macromolecules* **2011**, *44*, 1256–1260.

(56) Berlman, I. B. *Handbook of Fluorescence Spectra of Aromatic Molecules*, 2nd ed.; Academic Press: New York, 1971.

(57) Cross-checked against quinine bisulfate ($\Phi_f = 0.54$). By this method, our measured quantum yield of $\mathbf{oP(H)^2}$ (biphenyl) was in good agreement with the literature (0.18).

(58) Berlman, I. B. *J. Chem. Phys.* **1970**, *52*, 5616–5621.

(59) Momicchioli, F.; Bruni, M. C.; Baraldi, I. *J. Phys. Chem.* **1972**, *76*, 3983–3990.

(60) Heimel, G.; Daghofer, M.; Gierschner, J.; List, E. J. W.; Grimsdale, A. C.; Müllen, K.; Beljonne, D.; Brédas, J.-L.; Zojer, E. *J. Chem. Phys.* **2005**, *122*, 054501.